

Evaluation of Dosimetric Qualities of Ionization Chambers and Solid-State Detectors in Small Fields of a ^{60}Co Teletherapy Unit

Tanjina Akhter¹, Hossen Mohammad Jamil², Md Shakilur Rahman^{2*}, Sadeka Sultana Rubai¹, AKM Moinul Haque Meaze¹, Bushra Nafrin Sattar², KM Mahabub Morshed², Tanjim Siddiqua²

¹Department of Physics, University of Chittagong, Chittagong, Bangladesh

²Secondary Standard Dosimetry Laboratory (SSDL), Bangladesh Atomic Energy Commission (BAEC), Savar, Dhaka, Bangladesh

ARTICLE INFO

Article history:

Received : 28 July 2025

Received in revised form : 03 August 2025

Accepted : 25 September 2025

Available online : 01 October 2025

Key words:

^{60}Co Teletherapy Unit, Small Field, Absorbed dose rate to water (D_w), Field OFs; Microdiamond Solid-State Detector

doi: <https://doi.org/10.3329/bjamp.v16i2.84802>

Article Category: Radiotherapy Dosimetry

Corresponding author:

Md. Shakilur Rahman

shakilurssdl@baec.gov.bd

ABSTRACT

Radiotherapy is a medical procedure that eliminates cancer cells by destroying their DNA. Secondary Standard Dosimetry Laboratories (SSDLs) serve an important role in providing traceable calibrations at certain radiation qualities for use in radiation measuring systems. The aim of this study is to investigate the absorbed dose rate to water (D_w) at the reference depth ($z_{ref} = 5 \text{ g cm}^{-2}$), the absorbed dose rate to water at the depth of dose maximum (D_{max}), and the field output factors (OFs) for the different types of detectors (Farmer chamber type FC65-G, Semiflex chamber type 31010, Pinpoint 3D chamber type 31022, Diode E detector type 60017, and Microdiamond detector type 60019) in small fields of the ^{60}Co teletherapy unit. The dosimetric performances were investigated for a reference field size of $10 \times 10 \text{ cm}^2$, and for small field sizes of $5 \times 5 \text{ cm}^2$, $4 \times 4 \text{ cm}^2$, $3 \times 3 \text{ cm}^2$, and $2 \times 2 \text{ cm}^2$. The measurements were conducted in a Blue Phantom² 3D water phantom according to IAEA dosimetry protocol TRS 398 coupled with an electrometer (Dose-1 electrometer), at a source to detector distance of 100 cm. The D_w (z_{ref}) values for all five detectors are decreasing as the field size decreases from 10×10 to $2 \times 2 \text{ cm}^2$. Response variance is significant among detectors below a field size $4 \times 4 \text{ cm}^2$. Output factors (OFs) decrease as field size decreases, with all five detectors responding the same from $10 \times 10 \text{ cm}^2$ to $5 \times 5 \text{ cm}^2$. However, at small field sizes less than $3 \times 3 \text{ cm}^2$, there is significant variation across these detectors. Solid-state detectors are more compatible with small field sizes, making the Microdiamond detector more appropriate.

1. Introduction

Ionizing radiation is used to diagnose and treat illnesses, including cancer. Radiotherapy, also known as radiation oncology, is a medical specialty that uses high doses of radiation to destroy cancer cells and shrink tumors. This therapy kills cancer cells by damaging their DNA, causing them to either cease proliferating or die. However, radiation therapy does not immediately eliminate cancer cells, and they continue to die for weeks or months after treatment is completed [1,2]. In 1976, the IAEA and WHO established the network of SSDLs to standardize radiation readings. An SSDL is a laboratory approved by national authorities to provide radiation dosimetry traceability to the International System of Units (SI) for metrology users. The SSDLs play a significant role in delivering traceable calibrations at certain radiation qualities for use with radiation measurement devices [3].

Prasad Acharya *et al.* [4] analyzed the output dose from ^{60}Co teletherapy machines from 2012 to 2014 using actual dosimetry. The deviation was within the permissible limits of $\pm 2\%$ for each month calculation. The study concluded that the output dose delivered by the ^{60}Co Teletherapy Unit (TTU), Bhaktapur Cancer Hospital (BCH), Nepal, was consistent and accurate. It recommended continuous dosimetric analysis for continuous improvement. Healy *et al.* [5] examined the characteristics of ^{60}Co machines and linacs in LMIC settings. ^{60}Co machines have lower life-cycle costs, staffing levels, shielding requirements, and infrastructure. Linacs offer security arrangements and lack source exchange, while dosimetry differences make complex treatments easier. Local demand for curative and palliative treatments informs treatment complexity. A

radiotherapy department with both machines and linacs may cover all needs. Sustainability is the most important factor in choosing technology, as it ensures continuity in radiotherapy services. Mathuthu *et al.* [6] showed strong potential for ^{60}Co based teletherapy, with lower energy and penetration influencing intensity-modulated radiotherapy. Source head fluency can be modulated using secondary collimator jaw motion and a 3D physical compensator. Lauba & Wong [7] addressed the significance of correct absolute and relative dose measurements, with a focus on quality assurance measures in IMRT. Absolute dose measurements of intensity modulated fields using a 0.6 cm^3 Farmer chamber reveal substantial changes in dose levels of more than 6% at the iso-center of an IMRT treatment plan. In the same experiment, dosage levels assessed using a 0.015 cm^3 pinpoint ion chamber showed differences of no more than 2%. A diamond detector is found to be useful as an alternative to other detectors used for small field dosimetry, such as photographic and photochromic film, TLDs, or water-equivalent scintillation detectors, due to its high spatial resolution and water equivalency. Woodings *et al.* [8] characterized the influence of the PTW 60019 Microdiamond on a magnetic resonance linac (MRI-linac). Because of its tiny physical size, good signal-to-noise ratio, and approaching water equivalency, the PTW 60019 Microdiamond is close to an ideal detector for small field dosimetry. Gomà *et al.* [9] investigated a Microdiamond detector's performance in a scanned proton beam, and its potential usefulness in the dosimetric assessment of proton pencil beams. The detector reading was found to be linear with the absorbed dose to water (down to a few cGy), and the detector response is independent of both the dose rate (up to a few Gy/s) and the proton beam energy (within the clinically relevant energy range). Singh *et al.* [10] investigated the small field characteristics of the ^{60}Co source-based teletherapy system by altering the detector and source sizes. Square fields ranging in size from $1 \times 1\text{ cm}^2$ to $10 \times 10\text{ cm}^2$ were employed in their investigation. For experimental measurements, two distinct ionization chambers (SNC125c and Pinpoint) with varying sensitivity volumes were utilized, and Monte Carlo (MC) simulations were performed using the tool for particle simulation (TOPAS) version 3.5 toolkit. The current study found that chamber size has a substantial influence on the

assessment of tiny field characteristics, particularly OFs. Furthermore, source size is another element that has a considerable impact on beam profiles, limiting the usage of ^{60}Co teletherapy machines to field sizes less than $3 \times 3\text{ cm}^2$.

As part of quality control, the dosimetric performance of radiation detectors must be appropriately and precisely evaluated. The objective of the present study is to evaluate D_w at $z_{ref} = 5\text{ g cm}^{-2}$, the absorbed dose rate to water at D_{max} , and the OFs for the different types of detectors coupled with an electrometer (IBA Dose-1 electrometer) at a source to detector distance of 100 cm in small fields of ^{60}Co teletherapy unit. The dosimetric performances were investigated for a reference field size of $10 \times 10\text{ cm}^2$, and for small field sizes of $5 \times 5\text{ cm}^2$, $4 \times 4\text{ cm}^2$, $3 \times 3\text{ cm}^2$, and $2 \times 2\text{ cm}^2$. The measurements were conducted in a Blue Phantom² 3D water phantom according to IAEA dosimetry protocol TRS 398 [11].

2. Materials and Methods

The experimental procedure was performed by using IAEA dosimetry protocol TRS 398 [11] at the ^{60}Co Gamma Lab, SSDL, Bangladesh Atomic Energy Commission (BAEC), Savar, Dhaka, Bangladesh. The irradiations were performed by the Theratron Equinox External Beam Therapy System (^{60}Co Teletherapy Unit, Best Theratronics Ltd., Ottawa, Ontario, Canada). The absorbed dose rate to water (D_w) at the reference depth ($z_{ref} = 5\text{ g cm}^{-2}$), the absorbed dose rate to water at the depth of dose maximum (D_{max}), and the field OFs of gamma ray machines have been investigated for five detectors: Farmer chamber type FC65-G (IBA Schwarzenbruck, Germany), Semiflex chamber type 31010, Pinpoint 3D chamber type 31022, Diode E detector type 60017, and Microdiamond detector type 60019 (PTW, Freiburg, Germany) in a reference field size of $10 \times 10\text{ cm}^2$, and in small field sizes of $5 \times 5\text{ cm}^2$, $4 \times 4\text{ cm}^2$, $3 \times 3\text{ cm}^2$, and $2 \times 2\text{ cm}^2$. The measurements were performed with an electrometer (IBA Dose-1 electrometer) at a source to detector distance of 100 cm in small fields of ^{60}Co teletherapy unit in a 3D water phantom known as Blue Phantom² (IBA Schwarzenbruck, Germany) [12]. Table 1 presents several features of the detectors used in this study and Fig. 1 is a pictorial representation of measurement of absorbed dose rate to water using a Farmer chamber at SSDL, BAEC, Savar, Dhaka, Bangladesh.

Table 1: Technical specifications of the different detectors used in this work [12-13]

Specifications	Farmer Chamber Type FC65-G	Semiflex Chamber Type 31010	Pinpoint 3D Chamber Type 31022	Diode E Detector Type 60017	Microdiamond Detector Type 60019
Type of product	vented cylindrical ionization chamber	vented cylindrical ionization chamber	vented cylindrical ionization chamber	p-type silicon diode	synthetic single crystal diamond detector
Direction of incidence	radial	radial	radial, axial	axial	axial
Nominal sensitive volume	0.65 cm ³	0.125 cm ³	0.016 cm ³	0.00003 cm ³	0.000004 cm ³
Reference point	on chamber axis, 1.3 cm from chamber tip	on chamber axis, 0.45 cm from chamber tip	on chamber axis, 0.24 cm from chamber tip	on detector axis, 0.13 cm from detector tip	on detector axis, 0.1 cm from detector tip
Chamber voltage	+300 V nominal	+400 V nominal	+300 V nominal	0 V	0 V
Field size	5 × 5 cm ² ... 40 × 40 cm ²	3 × 3 cm ² ... 40 × 40 cm ²	2 × 2 cm ² ... 40 × 40 cm ²	1 × 1 cm ² ... 10 × 10 cm ²	1 × 1 cm ² ... 40 × 40 cm ²



Fig. 1: Pictorial representation of measurement of absorbed dose rate to water using a Farmer chamber at SSDL, BAEC, Savar, Dhaka, Bangladesh.

As per international protocol, all the detectors were calibrated in terms of the absorbed dose rate to water at the reference depth; hence, for the dosimetry, the k_Q factor

is considered 1. Also, all detectors were calibrated with the same electrometer (Dose-1); hence, the electrometer correction factor, k_{elec} , is considered 1.

D_w at the z_{ref} was calculated by the Equation- 2.1 [11]:

$$D_w(z_{ref}) = MN_{D,w} \tag{2.1}$$

Where, $N_{D,w}$ is the calibration factor in terms of absorbed dose to water for the dosimeter at the reference quality ⁶⁰Co.

M is the electrometer reading corrected for the polarity effect, ion recombination and air density (temperature and pressure) with the reference point of the chamber positioned at z_{ref} by the Equation- 2.2 [11]:

$$M = M_1 \times k_{elec} \times k_{TP} \times k_{pol} \times k_S \tag{2.2}$$

Where, M_1 = uncorrected electrometer reading;

k_{elec} = the electrometer correction factor;

k_{TP} = temperature and pressure correction factor;

k_{pol} = polarity correction factor;

k_S = ion recombination correction factor.

Here, these correction factors have been measured according to IAEA dosimetry protocol TRS 398 [11]. The values of $N_{D,w}$ of Farmer, Semiflex, and Pinpoint ionization chambers

are 4.856×10^7 Gy/c, 2.942×10^8 Gy/c, and 2.607×10^9 Gy/c respectively. For solid state detectors we multiplied M with the correction factors that have been found from the absorbed dose rate of Farmer for a reference field size of 10×10 cm². The value of the correction factor for Diode E is 0.101 Gy/nC. The value of the correction factor for Microdiamond is 1.298 Gy/nC. Thus, the absorbed dose rate to water at the reference depth, using Equation (2.1) for two solid-state detectors, was determined.

The absorbed dose rate to water at (D_{max}) was calculated by the Equation (2.3) [11]:

Here, $z_{max} = 0.5$ g cm⁻²

$$D_w(z_{max}) = \frac{D_w(z_{ref})}{PDD(z_{ref})} \times 100 \quad 2.3$$

The dosage at any depth along the central axis of the radiation beam, also known as the percentage depth dose (PDD), is one of the most often used quantities in dosimetry. The doses have been scanned using common control unit (CCU) which is close-packed unit completely software controlled combining controller and electrometers.

OFs of gamma ray machines is defined as the ratio of dose in water, D_w for a given beam collimator aperture, (A) at a reference depth, (d) to the dose at the same point and depth (d) for the reference collimator aperture, A_{ref} [11]. The reference collimator aperture or simply the reference field A_{ref} is usually chosen to be the 10×10 cm² collimator setting. The field output factors were calculated by the Equation (2.4) [11]:

$$OF = \frac{D_w(A, d)}{D_w(A_{ref}, d)} \quad 2.4$$

3. Results and Discussion

D_w at $z_{ref} = 5$ g cm⁻², the absorbed dose rate to water at D_{max} , and the OFs of gamma ray machines have been investigated for five detectors: Farmer chamber type FC65-G, Semiflex chamber type 31010, Pinpoint 3D chamber type 31022, Diode E detector type 60017, and Microdiamond detector type 60019 in a reference field size of 10×10 cm², and in small field sizes of 5×5 cm², 4×4 cm², 3×3 cm², and 2×2 cm² according to IAEA dosimetry protocol TRS-398 [11].

Several correction factors were applied for ambient conditions, polarity, and ion recombination. As per international protocol, all the detectors were calibrated in terms of the absorbed dose rate to water at the reference depth; hence, for the dosimetry, the k_Q factor is considered 1. Also, all detectors were calibrated with the same electrometer; hence, the electrometer correction factor, k_{elec} , is considered 1. The following Tables, 2, 3, 4, 5, and 6, are the representations of absolute dosimetry for Farmer, Semiflex, Pinpoint, Diode E, and Microdiamond detectors, respectively, using the IAEA TRS-398 protocol [11]. In Tables 2, 3, and 4 for ionization chambers, the correction factors, $D_w(z_{ref})$ at $z_{ref} = 5$ g cm⁻², $D_w(z_{max})$ at z_{max} , PDD at z_{ref} and OFs have been measured. In Tables 5 and 6, there is no need for correction factors for solid-state detectors like ionization chambers due to their physical construction. Therefore, in Tables 5 and 6 for solid-state detectors, $D_w(z_{ref})$ at $z_{ref} = 5$ g.cm⁻², the $D_w(z_{max})$ at z_{max} , the PDD at z_{ref} and the OFs have been measured.

Table 2: Absolute dosimetry according to IAEA TRS-398 for Farmer chamber

Field Size (cm ²)	$k_{T,P}$	k_{pol}	k_s	$D_w(z_{ref})$ Gy/min	PDD (z_{ref}) (%)	$D_w(z_{max})$ Gy/min	OF
10 × 10	1.009	1.000	1.000	0.97	80.4	1.21	1
5 × 5	1.009	1.001	1.000	0.89	76.7	1.15	0.95
4 × 4	1.009	1.001	1.000	0.85	75.4	1.13	0.93
3 × 3	1.010	1.001	1.000	0.76	73.8	1.03	0.85
2 × 2	1.010	1.001	1.000	0.56	72.1	0.78	0.64

Table 3: Absolute dosimetry according to IAEA TRS-398 for Semiflex chamber

Field Size (cm ²)	k _{TP}	k _{pol}	k _s	D _w (z _{ref}) Gy/min	PDD (z _{ref}) (%)	D _w (z _{max}) Gy/min	OF
10 × 10	1.021	0.993	1.000	0.98	80.59	1.26	1
5 × 5	1.021	0.992	1.000	0.89	77.23	1.16	0.95
4 × 4	1.022	0.992	1.000	0.87	75.69	1.15	0.94
3 × 3	1.022	0.991	1.000	0.83	74.31	1.11	0.91
2 × 2	1.022	0.997	1.000	0.67	71.78	0.93	0.77

Table 4: Absolute dosimetry according to IAEA TRS-398 for Pinpoint chamber

Field Size (cm ²)	k _{TP}	k _{pol}	k _s	D _w (z _{ref}) Gy/min	PDD (z _{ref}) (%)	D _w (z _{max}) Gy/min	OF
10 × 10	1.027	1.003	1.001	0.96	82.68	1.16	1
5 × 5	1.027	1.002	1.000	0.87	79.66	1.09	0.95
4 × 4	1.027	1.003	1.000	0.85	80.29	1.06	0.91
3 × 3	1.023	1.008	1.000	0.81	77.45	1.05	0.90
2 × 2	1.023	1.011	1.000	0.69	75.78	0.92	0.79

Data analysis for three ionization chambers (Farmer, Semiflex, and PinPoint) was performed using the derived correction factors in Tables 2, 3, and 4. Here, the deviation of the factors is extremely minor for all chamber field sizes from 10 × 10 cm² to 4 × 4 cm², although there are

deviations of k_{pol} and k_s in the small field size region below 4 × 4 cm². Farmer responses are the most stable of these three chambers, whereas Semiflex and PinPoint responses are less stable at field sizes smaller than 4 × 4 cm².

Table 5: Absolute dosimetry according to IAEA TRS-398 for Diode E detector

Field Size (cm ²)	D _w (z _{ref}) (Gy/min)	PDD (z _{ref}) (%)	D _w (z _{max}) (Gy/min)	OF
10 × 10	0.97	81.04	1.19	1
5 × 5	0.87	76.99	1.13	0.95
4 × 4	0.84	76.08	1.11	0.93
3 × 3	0.81	74.13	1.09	0.91
2 × 2	0.70	70.86	0.99	0.83

Table 6: Absolute dosimetry according to IAEA TRS-398 for Microdiamond detector

Field Size (cm ²)	D _w (z _{ref}) (Gy/min)	PDD (z _{ref}) (%)	D _w (z _{max}) (Gy/min)	OF
10 × 10	0.97	80.44	1.21	1
5 × 5	0.89	77.55	1.15	0.95
4 × 4	0.87	76.59	1.13	0.94
3 × 3	0.83	74.46	1.12	0.93
2 × 2	0.73	72.05	1.02	0.84

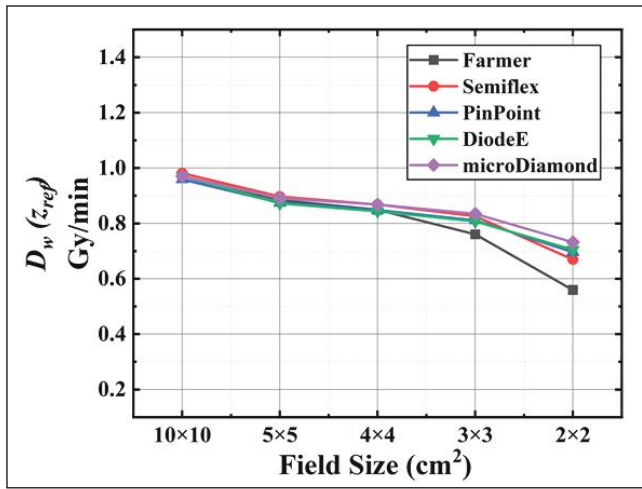


Fig. 2: $D_w(z_{ref})$ at z_{ref} of all five detectors as a function of the field size.

It is evident from the above graphical data representation (Fig. 2) - which is supported by Tables 2, 3, 4, 5, and 6, that $D_w(z_{ref})$ is falling for all five detectors at the same time as the field size is reducing from $10 \times 10 \text{ cm}^2$ to $2 \times 2 \text{ cm}^2$. There is a considerable response variance between all the detectors below field size $4 \times 4 \text{ cm}^2$, whereas the detector responses are almost identical within field sizes $10 \times 10 \text{ cm}^2$ and $4 \times 4 \text{ cm}^2$. The value of $D_w(z_{ref})$ for Farmer below field size $4 \times 4 \text{ cm}^2$ is steadily declining due to the volume effect, which is steeper than that of other ionization chambers (Semiflex & Pinpoint). This clearly demonstrates that for small field sizes under $3 \times 3 \text{ cm}^2$, solid state detectors (Diode E & Microdiamond) are more practical than ionization chambers. When it comes to the field size of $2 \times 2 \text{ cm}^2$, Microdiamond performs better than Diode E detector.

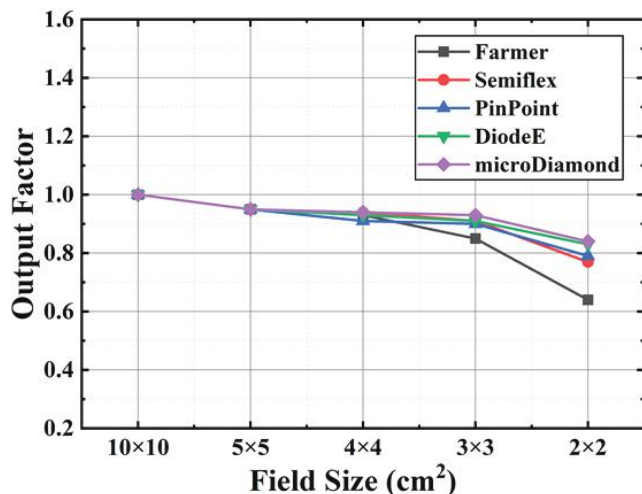


Fig. 3: Output factors of all five detectors as a function of the field size.

Fig. 3 depicts the measurement of output factors as field size decreases, as established in Tables 2, 3, 4, 5, and 6. From a field size of $10 \times 10 \text{ cm}^2$ to $5 \times 5 \text{ cm}^2$, all five detectors respond the same. There is little fluctuation in output factors from $5 \times 5 \text{ cm}^2$ to $3 \times 3 \text{ cm}^2$. However, at small field sizes of less than $3 \times 3 \text{ cm}^2$, there is significant variation across these five detectors. Because of the volume averaging effect and charged particle disequilibrium, ionization chambers (Farmer, Semiflex, and PinPoint) deviated more than solid-state detectors (Diode E, Microdiamond). There is charged particle equilibrium in large field sizes, and the volume impact is insignificant. As a result, measuring output factors in smaller fields necessitates dosimeters with better spatial resolution and smaller sizes. Due to its large sensitive volume, the Farmer chamber deviated more than other chambers. Therefore, for small field sizes, solid-state detectors are more compatible than ionization chambers; thus, the Microdiamond detector is more appropriate than other detectors in this case.

4. Conclusions

This study's goal is to assess dosimetric qualities of ionization chambers and solid-state detectors in small fields of ^{60}Co teletherapy unit according to IAEA TRS-398 protocol. The $D_w(z_{ref})$ values for all five detectors are decreasing as the field size decreases from $10 \times 10 \text{ cm}^2$ to $2 \times 2 \text{ cm}^2$. Response variance is significant among detectors below field size $4 \times 4 \text{ cm}^2$, but responses are nearly identical within field sizes $10 \times 10 \text{ cm}^2$ and $4 \times 4 \text{ cm}^2$. The Farmer detector's value is steadily declining due to the volume effect, which is steeper than other ionization chambers. For small field sizes under $3 \times 3 \text{ cm}^2$, solid-state detectors (Diode E & Microdiamond) are more practical than ionization chambers. OFs decrease as field size decreases, with all five detectors responding the same from $10 \times 10 \text{ cm}^2$ to $5 \times 5 \text{ cm}^2$. However, at small field sizes less than $3 \times 3 \text{ cm}^2$, there is significant variation across these detectors. Ionization chambers (Farmer, Semiflex, and Pinpoint) deviated more than solid-state detectors (Diode E, Microdiamond) due to volume averaging effect and charge particle disequilibrium. Large field sizes have charged particle equilibrium, and volume impact is insignificant. To measure OFs in smaller fields, dosimeters with better spatial resolution and smaller sizes are needed. Solid-state detectors are more compatible for

small field sizes, making the Microdiamond detector more appropriate. The investigation will assist in establishing future procedures for the advancement of small field dosimetry.

References

1. Podgoršak EB; Radiation Physics for Medical Physicists. Berlin, Heidelberg: Springer Berlin Heidelberg (2006).
2. National Cancer Institute (2025); External Beam Radiation Therapy for Cancer: Available at: <https://www.cancer.gov/about-cancer/treatment/types/radiation-therapy/external-beam>
3. International Atomic Energy Agency; Measurement Uncertainty, IAEA-TECDOC-1585, IAEA, Vienna (2008).
4. Acharya NP, Lamichhane TR and Jha B; Quality assurance with dosimetric consistency of a Co-60 teletherapy unit, J. Nep. Phy. Soci., 4(1): 88-92 (2017).
5. Healy BJ, Van Der Merwe D, Christaki KE and Meghziifene A; Cobalt-60 machines and medical linear accelerators: competing technologies for external beam radiotherapy, Clin. Onco., 29(2):110-115 (2017).
6. Mathuthu M, Mdziniso NW and Asres YH; Dosimetric evaluation of cobalt-60 teletherapy in advanced radiation oncology, Journal of Radiotherapy in Practice, 18(1) :88-92 (2019).
7. Laub WU and Wong T; The volume effect of detectors in the dosimetry of small fields used in IMRT, Medical Physics, 30(3): 341-347 (2003).
8. Woodings SJ, Wolthaus JW, van Asselen B, De Vries JHW, Kok JG, Lagendijk, JJW and Raaymakers BW; Performance of a PTW 60019 microDiamond detector in a 1.5 T MRI-linac, Physics in Medical Biology, 63(5) : 05NT04 (2018).
9. Gomà C, Marinelli M, Safai S, Verona-Rinati G and Würfel J; The role of a microDiamond detector in the dosimetry of proton pencil beams, Zeitschrift für Medizinische Physik, 26(1) :88-94 (2016).
10. Singh, A, Singh, G, Saini, A, Kinhikar, RA and Kumar, P; Small fields characterization of teletherapy cobalt-60 photon beam: An experimental and Monte-Carlo study. Measurement: Sensors, 25: 100595 (2003).
11. International Atomic Energy Agency; Absorbed dose determination in external beam radiotherapy, Technical Reports Series No. 398, IAEA, Vienna (2000).
12. iba-dosimetry (2022) Product Catalog – Radiation Therapy, Broadband Edition (Rev. 2).
13. PTW-Dosimetry (2016) Detectors Catalogue (English). Garching: PTW-Dosimetry.